hydrology

MDPI

Article

The Hydraulic Response of a Roadside Drainage System to Urban Trail Encroachment: Integrated HEC-RAS, Culvert, and Erosion-Stability Assessment

Ahmad J. Alzubaidi [1,2], Haneen H. Darwish [3], Mutaz M. Zoubi [4,5], Mohammed N. Assaf [6,*], Trung Do [7] and Nidal M. Hussein [2]

[1] Water Resources Unit, Crawford, Murphy & Tilly, Inc., Davenport, IA 52807, USA; aalzubaidi@cmtengr.com
[2] Department of Civil Engineering, Faculty of Engineering, University of Petra, Amman 11196, Jordan; nidal.hussein@uop.edu.jo
[3] Department of Civil Engineering, University of South Alabama, Mobile, AL 36688, USA; hhd2421@jagmail.southalabama.edu
[4] Department of Chemistry, The University of Jordan, Amman 11942, Jordan; m_zoubi@ju.edu.jo
[5] Chemical and Physical Analytical Laboratories, Jordan Atomic Energy Commission, Amman 11934, Jordan
[6] Department of Civil Engineering and Architecture, University of Pavia, 27100 Pavia, Italy
[7] Department of Civil, Coastal, and Environmental Engineering, University of South Alabama, Mobile, AL 36688, USA; trungdo@southalabama.edu
* Correspondence: mohammed.assaf@unipv.it or Ma.mohammed.assaf@gmail.com

Abstract

Urban trail construction can constrain existing roadside drainage corridors and alter water levels, flow velocity, culvert interaction, and erosion demand. This study evaluates a trail-constrained drainage retrofit in Moline, Illinois, USA, by linking changes in channel hydraulics to a proposed culvert-extension check and local lining demand. The study used StreamStats design hydrology, one-dimensional steady-flow HEC-RAS 6.5 outputs, HY-8 8.0.0 results, and HEC-15/IDOT riprap calculations. Existing and proposed conditions were compared at 24 matched HEC-RAS sections for the 10-, 25-, 50-, and 100-year events. Mean channel velocity decreased by 34.9–44.7%, while the median station-level water-surface-elevation (WSE) increase was 0.11–0.15 m; the corresponding mean WSE increase was 0.37–0.45 m because a small number of sections exhibited larger local changes. Velocity reductions were concentrated primarily within the reconstructed reaches, where mean reductions were about 54–56%; changes outside the reconstructed reaches were smaller and more variable. A targeted influence check excluding the anomalous downstream Station 2 found lower proposed-condition velocities at all 23 retained sections. A section-scale numerical sensitivity screening using plausible perturbations in roughness, discharge, and friction slope produced individual depth changes of less than 0.08 m at two representative reconstructed sections; a combined high-stage case increased depth by approximately 0.10–0.15 m without reversing the principal velocity-reduction pattern. The HY-8 calculation indicates that the proposed extension, 1.52 m in diameter, did not introduce an additional modeled restriction at the 100-year upstream design discharge of 5.89 m^3/s, while the 10-year HEC-15 check showed that the lining satisfied the adopted stability criterion at all 13 evaluated design stations. Interpretation remains conditional because the higher-return-period StreamStats flows are extrapolated, field calibration data are unavailable, the stair-like energy-dissipation structure is not explicitly represented, and the terminal box culvert may influence the downstream-most hydraulic response. The case study therefore provides a conditional engineering comparison of channel, culvert-extension, and erosion-protection responses rather than a field-validated prediction of retrofit performance.

Check for updates

Academic Editor: Hailong Yin

Received: 20 October 2026
Revised: 15 November 2026
Accepted: 20 November 2026
Published: 23 November 2026

Copyright: © 2026 by the authors. Licensee MDPI, Basel, Switzerland. This article is an open access article distributed under the terms and conditions of the Creative Commons Attribution (CC BY) license.

Keywords: urban drainage; stormwater management; HEC-RAS; roadside ditch; culvert hydraulics; riprap stability; hydraulic retrofit; trail infrastructure

1. Introduction

Urban stormwater infrastructure increasingly shares constrained rights-of-way with transportation, pedestrian, cycling, and utility infrastructure. This creates a practical design problem: a drainage corridor may need to preserve conveyance while its geometry, roughness, or structural controls are modified. Recent urban-drainage studies have emphasized system-level hydraulic assessment rather than isolated pipe or capacity checks [1–6]. Roadside channels are especially relevant because they can simultaneously convey runoff, control local water levels, and concentrate erosive stresses [7–9].

Hydraulic modeling provides a practical basis for comparing existing and proposed infrastructure when the dominant flow path is well defined. Recent HEC-RAS applications have examined urban flooding, roadside drainage, transportation crossings, and the sensitivity of model results to terrain and model dimensionality [8–15]. These studies also show that local results can depend on topographic representation, roughness, boundary treatment, and the degree to which abrupt structures are represented explicitly [12–15].

Data limitations remain important in small urban catchments. Field observations are often sparse, and regional or transferred hydrologic parameters may therefore be used as design inputs [16–19]. In Illinois, StreamStats regional regression provides peak-flow quantiles and associated uncertainty methods for ungaged locations, but its recommended application domain must be respected [20]. Where a drainage area falls outside that range, an independent plausibility check and an explicit uncertainty statement are warranted.

Hydraulic conveyance also cannot be separated from erosion protection. Channel shear depends on depth, slope, hydraulic radius, and lining properties, so lower velocity does not automatically imply lower local protection demand. Recent work on stormwater controls and watershed erosion similarly indicates that local hydraulic or sediment response can remain spatially concentrated even when system-level metrics improve [21,22]. The broader infrastructure-sustainability literature further emphasizes the importance of connecting hydraulic serviceability with long-term resilience [23].

The problem addressed here is how to assess channel, culvert-extension, and lining performance together when trail construction constrains an existing roadside drainage corridor. The case study is Phase II of the River-to-River Corridor Trail in Moline, Illinois, USA, where the proposed trail encroaches on a steep roadside ditch and requires local ditch reconstruction, extension of an existing culvert outlet, and replacement of deteriorated concrete lining with riprap [24].

The objectives were to (1) quantify changes in WSE, channel velocity, Froude number, flow area, top width, and energy-grade slope under 10-, 25-, 50-, and 100-year design events; (2) distinguish direct hydraulic changes within reconstructed reaches from propagated changes outside those limits; (3) diagnose the anomalous behavior of the downstream-most numerical section and quantify its influence on reach summaries; (4) evaluate the HY-8 check of the proposed 60 in extension; and (5) evaluate the 10-year riprap lining design against HEC-15/IDOT criteria.

2. Methodology

2.1. Study Area and Drainage Setting

Phase II of the River-to-River Corridor Trail follows portions of 19th Street and 27th Street in Moline, Rock Island County, Illinois, USA (Figure 1). The trail has a nominal width

of 3.05 m (10 ft). The hydraulic analysis focused on the roadside ditch along the west side of 27th Street [24].

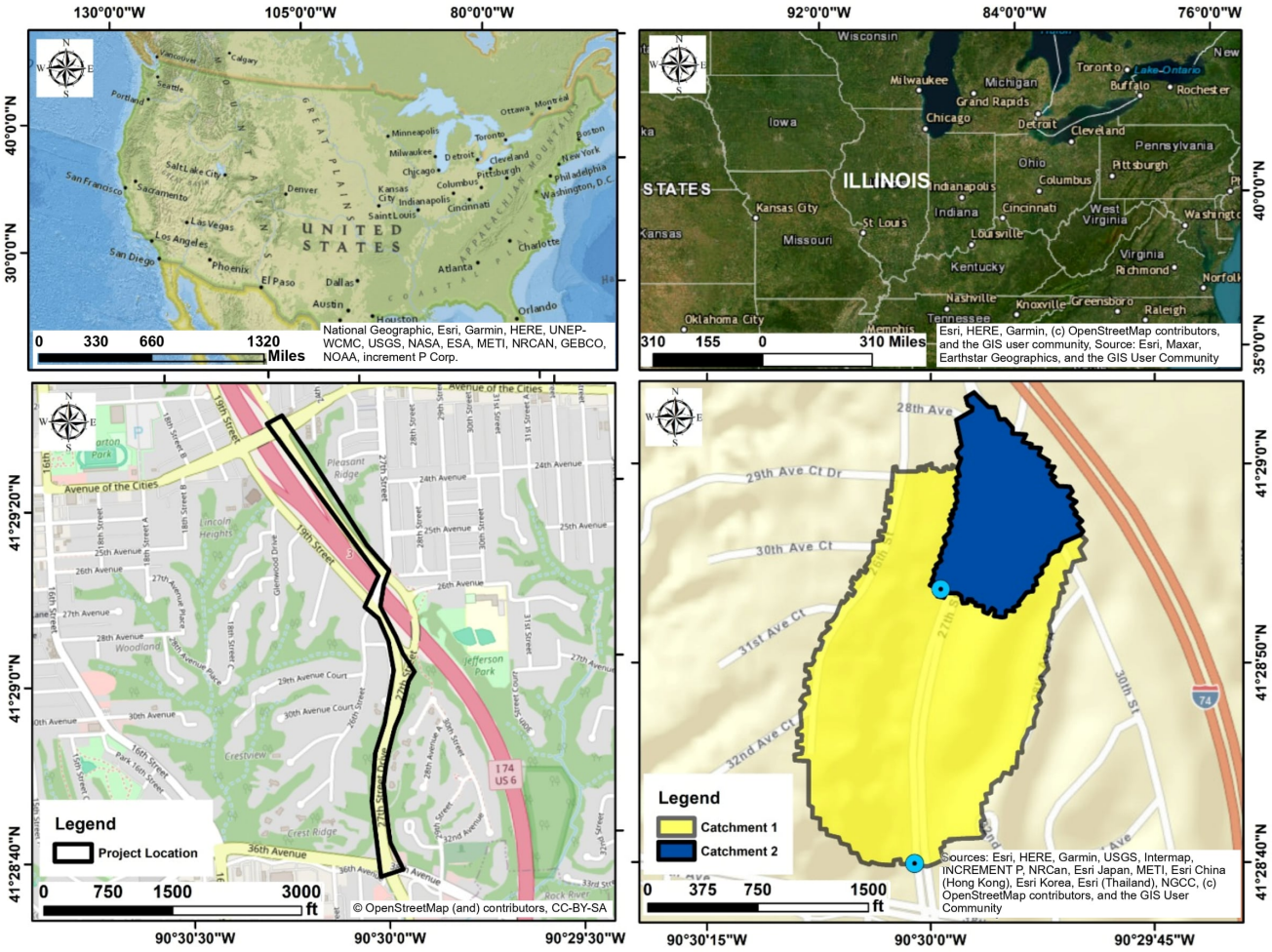

Figure 1. Study area, River-to-River Trail corridor, and the two StreamStats(version 4.19.4) analysis areas. The downstream analysis area represents the larger cumulative contributing area.

The analyzed ditch is approximately 405 m (1330 ft) long with an average longitudinal slope of about 3%. Existing drainage connections include a 1.07 m (42 in) circular culvert near STA 230+68, a 0.61 m (24 in) culvert near STA 234+01, and a 0.30 m (12 in) storm sewer near STA 241+03. The ditch discharges toward an 8 ft x 3 ft box culvert near STA 244+02. The principal reconstructed reaches are STA 229+15-233+10 and STA 237+06-242+38 [24].

2.2. Engineering Provenance and Assessment Framework

The study design criteria distinguish three relevant checks: the roadside ditch and culvert design frequency is 50 years; ditch lining is designed for the 10-year event using HEC-15 [25] and IDOT Drainage Manual Section 9.500 [26]; and the study analysis additionally reports 100-year WSE/freeboard and a 100-year HY-8 verification of the proposed 60 in extension [24]. Figure 2 summarizes the system, reconstruction limits, hydraulic structures, and flow-application locations.

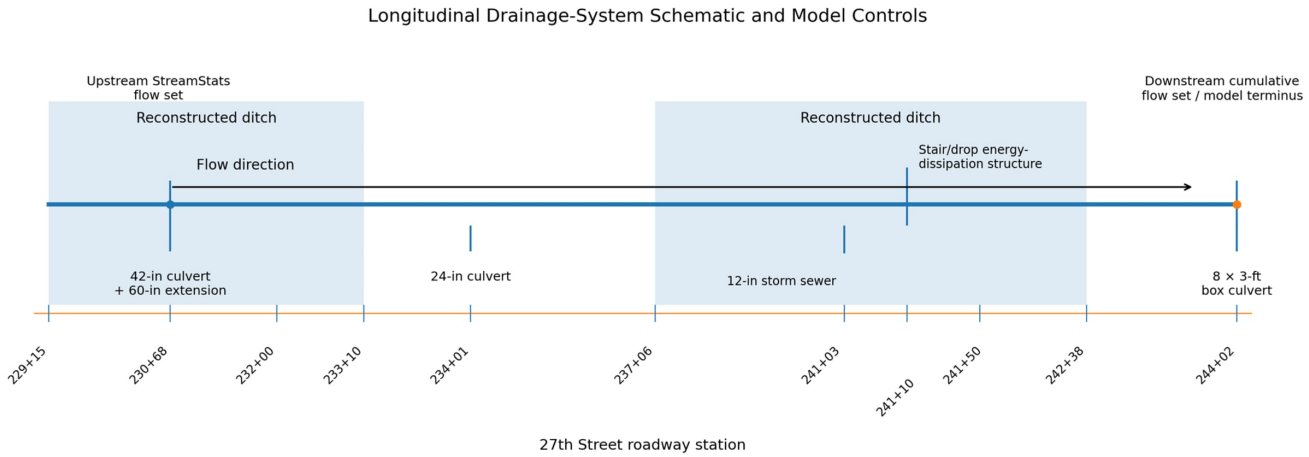

Figure 2. Longitudinal drainage-system schematic showing the reconstructed ditch reaches, lateral conduits, stair/drop structure, terminal box culvert, and the two StreamStats flow locations. Roadway stationing is from the study plans.

2.3. Data Sources, Geometry, and Model Setup

The study used survey information and available LiDAR to construct existing and proposed terrain surfaces in RAS Mapper (Table 1). A total of 28 existing and 25 proposed cross-sections were developed at approximately 15.2 m (50 ft) spacing. The numerical output contains 27 existing and 24 proposed numerical river stations plus a structure marker; 24 numerical stations are common to both scenarios and form the matched comparison. Manning roughness coefficients were assigned by local channel, lining, pavement, and vegetation zones and varied among cross-sections according to the model surface zoning. The assigned values are summarized in Appendix B and are consistent with the open-channel and floodplain roughness framework described in IDOT Drainage Manual Chapter 5 [26]. Representative hydraulic geometry is also provided in Appendix B. Supporting HEC-RAS longitudinal profiles, representative cross-sections, downstream-control geometry, and project plan/profile sheets are provided in the Supplementary Materials (Figures S1–S5).

Table 1. Hydraulic model setup, governing study criteria, and reproducibility notes.

Item	Setting/Criterion
HEC-RAS software	Version 6.5; 1D steady flow [27]
Cross-sections	~15.2 m spacing; 28 existing/25 proposed reported; 24 common numerical stations used for comparison
Roughness	Actual model assignments by surface/lining zone: concrete or paved zones approximately 0.013; earthen/grass channel 0.030–0.035; stair/drop transition 0.025–0.030; riprap 0.035–0.040; riprap/gabion 0.040–0.045; vegetated/grass overbank 0.040–0.050. Individual cross-sections retain locally zoned values as shown in the source HEC-RAS sections [26]; see Appendix B.
Transition losses	Standard HEC-RAS gradual-transition values were used where applicable; the reference values are 0.1 for contraction and 0.3 for expansion [27]
Boundary conditions	Normal-depth boundary slopes: upstream 0.030 ft/ft; downstream 0.0245 *ft/ft* (existing) and 0.020 *ft/ft* (proposed), applied with Manning normal-depth treatment [27].
Flow regime	Predominantly supercritical, with local near-critical/subcritical sections evident in detailed outputs
Hydrologic forcing	Two total StreamStats flow sets: upstream analysis area and downstream cumulative analysis area [20]
Unmodeled structure	Stair-like energy-dissipation structure at STA 241+10 omitted from the 1D channel geometry; quantitative screening is provided in Sections 3.8 and 4.3.
Study acceptance checks	50-year ditch/culvert design; 10-year lining design; additional 100-year WSE/freeboard and 60 in extension checks. Higher-return-period StreamStats discharges are adopted design inputs rather than independently validated flood estimates.

The assigned roughness ranges are the model inputs. Within a reach, individual cross-sections used values from the stated range according to local lining and vegetation. Standard gradual-transition coefficients of 0.1 for contraction and 0.3 for expansion were used where applicable in the one-dimensional steady-flow calculations [27].

2.4. Existing and Proposed Drainage Configurations

The proposed trail occupies part of the existing ditch corridor. The reconstructed channel follows the existing alignment where practicable, with foreslopes adjusted to approximately 3H:1V or 2H:1V and an approximately 2% longitudinal grade through much of the reconstructed reach. Riprap replaces deteriorated concrete lining over the reconstructed limits, and a gabion treatment is provided near STA 241+50 [24].

Trail encroachment would obstruct the outlet of the existing 42 in crossing culvert. The study therefore extends the outlet using a 1.52 m (60 in) concrete pipe from approximately STA 230+67.9 to STA 232+00. The 24 in culvert and 12 in storm sewer remain intermediate lateral connections within the larger downstream contributing drainage system.

2.5. Hydrologic Design Flows and Plausibility Screening

USGS StreamStats was used at an upstream analysis point near the 42 in culvert connection and a downstream point near the terminal box culvert. The delineated areas are approximately 0.021 mi^2 (0.054 km^2) and 0.077 mi^2 (0.199 km^2), respectively. The downstream area is the larger cumulative drainage area.

$$P = 1/T \quad (1)$$

$$P(\%) = 100/T \quad (2)$$

Both drainage areas fall below the recommended range for the applicable Illinois regional regression equation; StreamStats therefore identifies the estimates as extrapolated with unknown error [20,24]. As an independent order-of-magnitude check, the inlet calculations give a 10-year, 5 min rainfall intensity of approximately 7.2 in/h. Using the Rational Method, $Q = C\,i\,A$, for the 13.44-acre upstream area and a plausible urban runoff-coefficient range $C = 0.80–0.95$ gives approximately 77–92 cfs, compared with the StreamStats 10-year estimate of 105 cfs. This comparison supports only the order of magnitude of the 10-year input. The 25-, 50-, and 100-year StreamStats values are treated as adopted design discharges rather than independently validated flood estimates. The 50-year event is the principal ditch/culvert design event, while the 100-year event is used as an additional hydraulic verification/stress scenario.

$$Q = C\,i\,A \quad (3)$$

2.6. HEC-RAS Hydraulic Modeling

Open-channel hydraulics were evaluated in HEC-RAS 6.5 using separate existing and proposed one-dimensional steady-flow geometries [24,27]. The study states that supercritical flow prevailed over most of the steep ditch, but detailed outputs include local near-critical and subcritical sections; the reach is therefore described here as predominantly supercritical with local regime transitions.

Two total flow sets were used. The upstream set represents the beginning of the analyzed ditch/42 in culvert connection, while the downstream set represents the larger cumulative contributing area near the terminal outlet. The intermediate 24 in and 12 in connections are therefore components of the cumulative downstream drainage system rather than separately added StreamStats hydrographs.

Normal-depth boundary conditions were specified using an upstream friction slope of $0.030\,ft/ft$ (3.0%) and downstream slopes of $0.0245\,ft/ft$ (2.45%) for the existing condition and

0.020 *ft*/*ft* (2.0%) for the proposed condition. In HEC-RAS, normal depth is calculated from Manning conveyance using the user-entered friction slope [27]. A generic culvert structure marker occurs near the downstream end of the detailed HEC-RAS output, but the available model documentation does not permit verification of whether its geometry and parameters correspond completely to the terminal 8 ft × 3 ft box culvert at STA 244+02. The stair-like energy-dissipation structure at STA 241+10 was omitted from the 1D channel geometry; the local ditch slope changes from approximately 1.3% to 10%. These two downstream controls are therefore evaluated through separate engineering screening calculations and are treated as local sources of uncertainty.

2.7. Proposed 60 in Culvert-Extension Hydraulic Check

The HY-8 8.0.0 calculation specifically evaluates the proposed 60 in circular concrete extension downstream of the existing 42 in crossing culvert [24,28]. The available output spans 147–208 cfs, corresponding to the 25-, 50-, and 100-year upstream StreamStats events with intermediate increments.

The check should not be interpreted as a new capacity analysis of the existing 42 in barrel or of the two pipes as an independently modeled series system. Its purpose was to determine whether the larger downstream extension would introduce an additional modeled restriction under the study design check.

$$Q_extension \geq Q_100 \quad (4)$$

2.8. Riprap and Erosion-Stability Assessment

The study lining design uses the 10-year event, FHWA HEC-15, Third Edition, and IDOT Drainage Manual Section 9.500 [24–26]. Thirteen design/control stations within the reconstructed riprap reaches were retained in the detailed worksheet. These are study design stations rather than a statistical sample of every HEC-RAS section.

The applied/design shear was calculated using the local section/bed slope S, while the HEC-RAS energy-grade slope is reported separately. The lining check therefore uses the HEC-15 form tau_d = gamma d S, with permissible shear and safety factor evaluated independently [25].

$$tau_d = gamma\ d\ S \quad (5)$$

$$tau_p = F^* (gamma_s - gamma)\ D50 \quad (6)$$

$$tau_p \geq SF\ tau_d \quad (7)$$

The HEC-15 worksheet uses the Reynolds number-dependent Shields parameter F* and safety factor SF, with the calculation showing F* = 0.047 and SF = 1.0 at the lower limit, F* = 0.15 and SF = 1.5 at the upper limit, and interpolation between the limits [24,25]. RR4, RR5, and RR6 are IDOT riprap gradation designations; the detailed study worksheet uses selected D50 values of 0.75 ft (0.229 m), 1.00 ft (0.305 m), and 1.50 ft (0.457 m), respectively, at the design stations.

2.9. Matched-Section Comparative Analysis

Twenty-four numerical HEC-RAS stations are common to both scenarios. For each variable X, the station-level modeled difference was defined as:

$$Delta\ X_i = X_proposed,i - X_existing,i \quad (8)$$

The primary summaries are the median, interquartile range (IQR), station-level range, and direction of change. Means are retained as secondary design-summary statistics. No

population-level significance test is used because adjacent hydraulic sections are serially connected deterministic model outputs rather than independent random observations.

$$\text{Delta X_mean}(\%) = 100\ (\text{Xbar_proposed} - \text{Xbar_existing})/\text{Xbar_existing} \quad (9)$$

A standardized paired difference, d_z = mean(Delta X_i)/s_d, is retained only as a descriptive scale indicator and is not interpreted as population-level statistical inference.

$$\text{d_z} = \text{mean}(\text{Delta X_i})/\text{s_d} \quad (10)$$

For spatial interpretation, roadway stationing was taken directly from the station labels shown on the source HEC-RAS cross-section plots rather than inferred from HEC-RAS river-station distance. The resulting source-based crosswalk places 15 of the 24 common numerical sections within the two reconstructed reaches and 9 outside them. This separation distinguishes direct reconstruction effects from smaller propagated changes. The complete HEC-RAS river-station/roadway-station crosswalk is provided in Appendix B.

2.10. Station 2 Influence and Internal Verification

Station 2 is the downstream-most numerical section adjacent to the terminal boundary. Its hydraulic response is strongly non-monotonic under existing conditions, so it is retained in the complete dataset but evaluated separately using WSE, hydraulic depth, flow area, top width, velocity, and Froude number. A generic HEC-RAS culvert marker at RS 94 lies immediately upstream of Station 2, while the downstream end is controlled by the specified normal-depth boundary. Because the available information does not uniquely separate boundary, local-structure, geometry, and regime-transition effects, Station 2 is not used as a representative interior-reach section.

Internal consistency was also assessed by checking whether representative values of Q and VA were approximately equal, reviewing the HEC-15 equations against the detailed worksheet, and comparing model-section locations with study stationing. These are verification/consistency checks, not field calibration or validation.

2.11. Screening Sensitivity and Model Limitations

A section-scale numerical sensitivity screening was performed at two representative reconstructed locations, STA 232+00 and STA 239+00, using the hydraulic geometry and 10-year lining-design outputs. Each section was represented by an equivalent trapezoidal geometry reproducing its reported flow area, top width, and water depth. Manning conveyance was calibrated to the baseline condition and then recomputed for roughness perturbations of ±10%, discharge perturbations of ±20%, and friction-slope perturbations of ±20%. A combined high-stage case used +10% roughness, +20% discharge, and -20% slope. Changes in water depth were interpreted as equal and opposite changes in freeboard for a fixed bank elevation, and applied boundary shear was evaluated from tau = gamma d S. The ±20% discharge range is an engineering stress-test interval rather than a StreamStats confidence interval. Appendix B provides the equations, baseline values, and results.

The principal limitations are: (i) StreamStats extrapolation outside the recommended drainage-area range; (ii) absence of observed event data for calibration or independent validation; (iii) incomplete terrain metadata; (iv) inability to reproduce a full parameter-by-parameter HEC-RAS rerun from the available model files; (v) omission of the stair-like energy-dissipation structure from the 1D channel geometry; and (vi) uncertainty in the exact representation and hydraulic parameterization of the terminal box culvert. Relative existing–proposed differences remain useful for scenario comparison because the same adopted forcing and computational framework were used, but absolute WSE, velocity, freeboard, and shear values remain conditional on geometry, roughness, hydrologic input, boundary treatment, and local structural controls.

3. Results

3.1. Design Flows

The adopted 10- to 100-year StreamStats design discharges are listed in Table 2. The Rational Method screening for the upstream area produced a 10-year discharge of approximately 77–92 cfs for C = 0.80–0.95, compared with the StreamStats value of 105 cfs. This comparison supports the order of magnitude of the 10-year input but does not provide an independent validation or uncertainty bound for the 25-, 50-, or 100-year discharges. Results for the higher-return-period events are therefore interpreted as conditional responses to the adopted design flows.

Table 2. Design peak discharges used in the hydraulic comparison.

Return Period (yr)	AEP (%)	Upstream Q, cfs (m^3/s)	Downstream Q, cfs (m^3/s)
10	10	105 (2.97)	226 (6.40)
25	4	147 (4.16)	310 (8.78)
50	2	176 (4.98)	370 (10.48)
100	1	208 (5.89)	437 (12.37)

3.2. Matched Hydraulic Response

Across all 24 sections, mean velocity decreased by 34.9%, 44.3%, 44.7%, and 39.2% for the 10-, 25-, 50-, and 100-year events, respectively (Table 3, Figure 3). The median velocity change ranged from −2.26 to −3.73 m/s. Median WSE increases were much smaller than the corresponding arithmetic means because a limited number of reconstructed sections exhibited larger WSE shifts. The largest modeled WSE rise occurred at HEC-RAS Station 1307 (approximately roadway STA 231+50), reaching about 2.14–2.19 m across the four events.

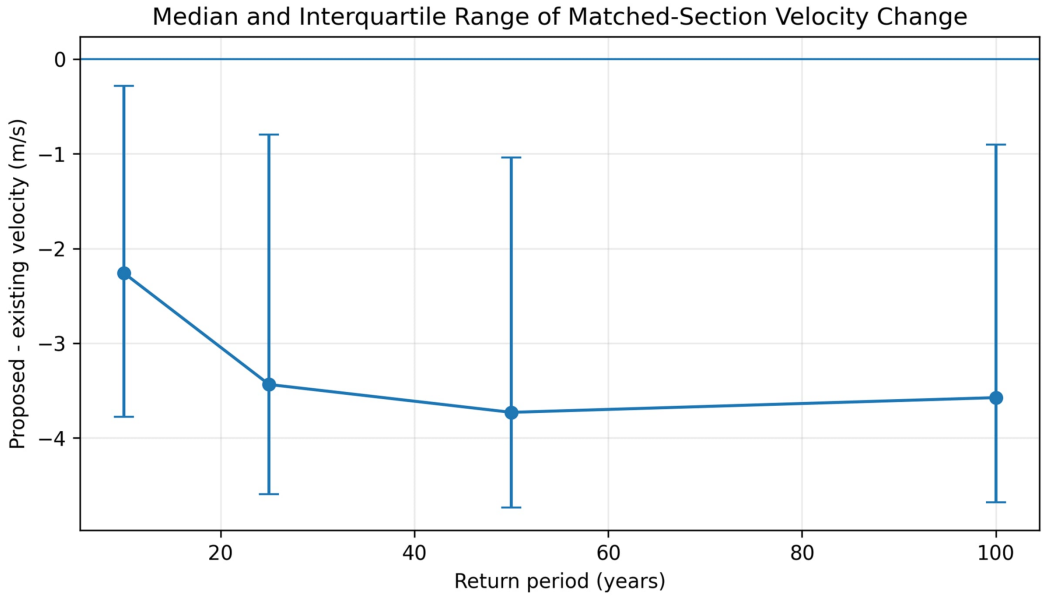

Figure 3. Median and interquartile range of proposed-minus-existing channel-velocity change across the 24 matched sections. Negative values indicate lower proposed velocity.

Table 3. Matched-section hydraulic response. Median values are followed by the IQR in parentheses; means are retained as secondary design-summary statistics.

RP (yr)	Median ΔWSE, m (IQR)	Maximum ΔWSE	Mean Velocity Ex/Pr (m/s)	Mean Velocity Change (%)	Median ΔV, m/s (IQR)	Median ΔFr
10	0.11 (0.02 to 0.81)	2.14 at STA 231+50	6.03/3.93	−34.9	−2.26 (−3.78 to −0.28)	−1.25
25	0.14 (0.04 to 0.83)	2.17 at STA 231+50	7.58/4.22	−44.3	−3.44 (−4.59 to −0.80)	−1.34
50	0.13 (0.04 to 0.85)	2.18 at STA 231+50	7.96/4.40	−44.7	−3.73 (−4.74 to −1.04)	−1.32
100	0.15 (0.04 to 0.86)	2.19 at STA 231+50	7.47/4.54	−39.2	−3.57 (−4.68 to −0.90)	−1.27

3.3. Reconstructed Versus Outside-Reach Response

The velocity reduction was concentrated primarily within the reconstructed reaches (Table 4, Figure 4). Mean velocity reductions there were approximately 54.4–56.2% across the four events, with median WSE increases of about 0.78–0.85 m. The nine sections outside the reconstructed limits showed substantially smaller and more variable changes, including a 4.2% reduction in the 100-year mean velocity. The segmented results indicate that the strongest hydraulic response is associated directly with the reconstructed geometry and lining, while changes outside those limits reflect propagated hydraulic effects.

Table 4. Hydraulic response inside the reconstructed reaches versus that in matched sections outside the reconstruction limits.

RP	Section Group	n	Ex Mean V (m/s)	Pr Mean V (m/s)	Mean ΔV (%)	Median ΔV (m/s)	Median ΔWSE (m)
10	Reconstructed	15	6.54	2.98	−54.4	−3.61	0.78
10	Outside	9	5.19	5.5	6	−0.14	0.01
25	Reconstructed	15	7.24	3.23	−55.4	−4.02	0.81
25	Outside	9	8.13	5.87	−27.9	−0.44	0.03
50	Reconstructed	15	7.65	3.38	−55.8	−4.35	0.8
50	Outside	9	8.47	6.11	−27.9	−0.61	0.05
100	Reconstructed	15	8.04	3.53	−56.2	−4.64	0.85
100	Outside	9	6.51	6.23	−4.2	−0.6	0.04

3.4. Station 2 Diagnostic and Influence Check

Station 2 shows a non-monotonic change in existing-condition velocity from 3.43 m/s (10-year) to 24.27 and 23.77 m/s (25- and 50-year) and then to 2.56 m/s (100-year) (Table 5). Existing hydraulic depth changes from approximately 1.47 m to 0.46, 0.54, and 2.01 m across the same events, while flow area changes from 2.19 m^2 to 0.45, 0.54, and 13.71 m^2, and the Froude number changes from 1.10 to 13.22, 12.07, and 0.66. The proposed results are more regular, with hydraulic depth increasing from approximately 0.41 to 0.55, 0.63, and 0.80 m. A generic HEC-RAS culvert marker at RS 94 lies immediately upstream of Station 2, and the section is adjacent to the downstream normal-depth boundary. The anomaly is therefore consistent with a local control/regime transition, but the available information does not uniquely distinguish boundary-condition effects, local-structure effects, geometry, and numerical regime switching.

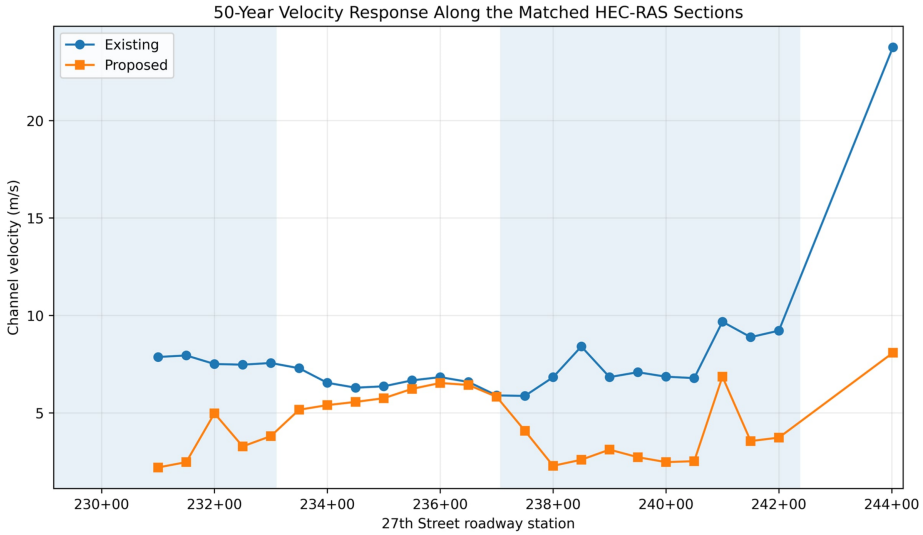

Figure 4. Existing and proposed channel velocity for the 50-year event along the matched sections. Shaded bands identify the two reconstructed ditch reaches.

Table 5. Diagnostic hydraulic output at downstream HEC-RAS Station 2.

RP	Ex V (m/s)	Pr V (m/s)	Ex Area (m2)	Pr Area (m^2)	Ex Fr	Pr Fr	ΔWSE (m)
10	3.43	8.80	2.19	0.80	1.10	4.57	−1.05
25	24.27	8.16	0.45	1.23	13.22	3.63	0.09
50	23.77	8.08	0.54	1.51	12.07	3.33	0.10
100	2.56	7.05	13.71	2.11	0.66	2.58	−1.21

After exclusion of Station 2, proposed velocity remained lower at all 23 retained sections for each design event, with mean reductions of approximately 39.6–42.3% (Table 6). This confirms that the interior-section velocity pattern is not created by the anomalous boundary-adjacent value; it does not establish robustness to uncertain roughness, discharge, or boundary slopes.

Table 6. Targeted Station 2 influence check for channel velocity.

RP	Existing Mean V (m/s)	Proposed Mean V (m/s)	Mean Change (%)	Sections Lower
10	6.15	3.71	−39.6	23/23
25	6.85	4.05	−40.9	23/23
50	7.27	4.24	−41.6	23/23
100	7.68	4.43	−42.3	23/23

3.5. Water-Surface Response and Freeboard

The proposed geometry produced higher WSE at most matched sections, but the magnitude was strongly location-dependent (Figure 5). Median increases were about 0.11–0.15 m, while the largest local increase was about 2.19 m at the upstream reconstructed reach. Because the channel was regraded, absolute WSE differences include changes in local geometry/elevation and should not be interpreted as a uniform increase in flow depth. The 100-year design check indicates that WSE remained within the proposed ditch with more than 0.91 m (3 ft) of freeboard [24]. In the section-scale sensitivity screening, the combined high-stage case increased representative water depths by approximately 0.105 and 0.150 m; at fixed bank elevations, the same increments represent corresponding reductions in freeboard. This screening does not replace a full model rerun but provides a quantitative scale for parameter-related uncertainty.

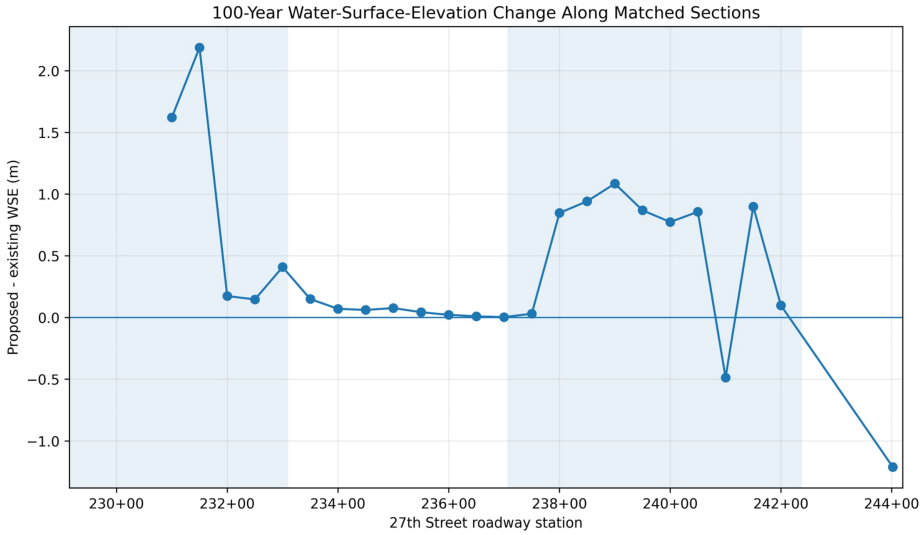

Figure 5. Proposed-minus-existing WSE change for the 100-year event along the matched sections. Shaded bands identify the reconstructed reaches.

3.6. Proposed 60 in Extension Check

The HY-8 run includes the 100-year upstream design flow. The proposed 60 in extension did not introduce an additional modeled restriction in that component check; the calculation does not independently establish the capacity of the existing 42 in barrel or of the complete 42/60 in system. HY-8 reports an outlet velocity of 16.49 ft/s (5.03 m/s), as shown in Table 7. The receiving ditch at STA 232+00 has a modeled channel velocity of 15.87 ft/s (4.84 m/s) in the 10-year HEC-15 lining calculation. These velocities are of similar magnitude but represent different hydraulic design checks; this comparison is therefore not used to infer that one condition is automatically conservative relative to the other. The final controlling riprap lining calculation dated 15 March 2024 adopts RR6 with D50 = 1.50 ft (18 in; 0.457 m) at STA 232+00. Applied shear is 13.85 lb/ft^2 (663.1 Pa), permissible shear is 23.09 lb/ft^2 (1105.6 Pa), and the adopted safety factor is 1.50, giving an SF-adjusted stability ratio of 1.11. The adopted lining therefore satisfies the HEC-15 shear criterion at this design station, although this receiving-channel lining check is not a coupled outlet-jet scour analysis, as shown in Table 7.

Table 7. HY-8 output for the proposed 60 in extension at the 100-year upstream design discharge.

Variable	Result
Design discharge	208 cfs (5.89 m^3/s)
Headwater elevation	644.30 ft (study datum)
Inlet-control depth	8.80 ft (2.68 m)
Outlet-control depth	5.70 ft (1.74 m)
Normal depth	2.63 ft (0.80 m)
Critical depth	4.11 ft (1.25 m)
Outlet depth	2.98 ft (0.91 m)
Tailwater depth	1.43 ft (0.44 m)
Outlet velocity	16.49 ft/s (5.03 m/s)

3.7. Shear Stress and Riprap Stability

All 13 study design/control stations satisfy the adopted worksheet criterion, but the margins are not uniform. The smallest SF-adjusted stability ratios are 1.06 at STA 232+50 and STA 233+00 and 1.11 at STA 232+00. These locations warrant the greatest caution because hydrologic and hydraulic uncertainty can consume a relatively small design margin. Table 8 summarizes the complete 10-year lining checks.

Table 8. Detailed 10-year riprap lining checks. The final column is the SF-adjusted stability ratio tau_p/(SF tau_d).

Station	Applied Shear (Pa)	Permissible Shear (Pa)	SF	Riprap	D50 (m)	SF-Adjusted Ratio
232+00	663.1	1105.6	1.500	RR6	0.457	1.11
232+50	248.5	313.1	1.184	RR4	0.229	1.06
233+00	163.3	173.3	1.000	RR4	0.229	1.06
237+00	83.8	228.9	1.074	RR4	0.229	2.54
237+50	107.3	362.9	1.250	RR4	0.229	2.71
238+00	120.7	173.3	1.000	RR4	0.229	1.44
238+50	147.5	257.6	1.111	RR4	0.229	1.57
239+00	123.5	277.2	1.137	RR4	0.229	1.97
239+50	126.4	248.5	1.099	RR4	0.229	1.79
240+00	137.9	200.6	1.036	RR4	0.229	1.40
240+50	159.9	257.6	1.112	RR4	0.229	1.45
241+50	351.9	554.9	1.320	RR5	0.305	1.19
242+00	195.4	230.8	1.000	RR5	0.305	1.18

The final detailed riprap lining calculation dated 15 March 2024 is used as the controlling source for the station-specific design values. At STA 232+00, the final calculation adopts RR6 with D50 = 1.50 ft (18 in), superseding the earlier 15 in plan/profile notation. At STA 232+50, the final calculation uses RR4 with D50 = 0.75 ft, while STA 241+50-242+00 uses RR5 with D50 = 1.00 ft. These final station-specific values are used throughout the hydraulic interpretation, as shown in Figure 6.

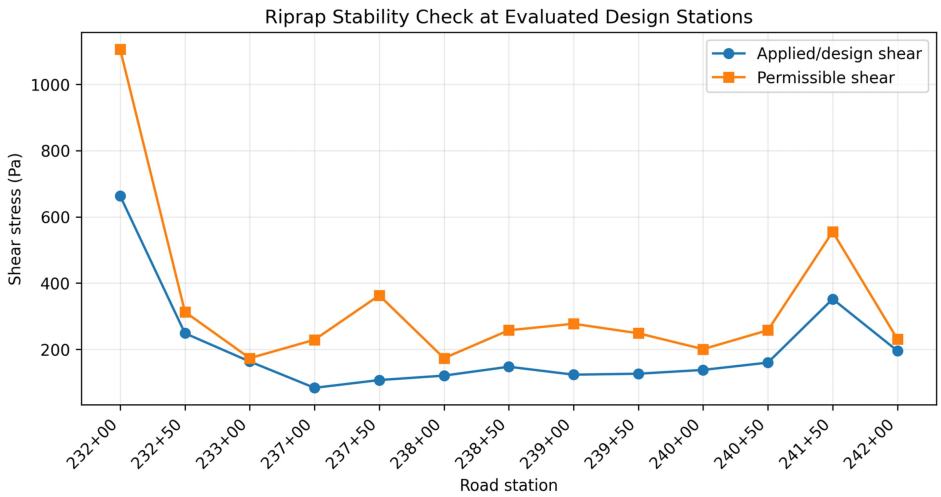

Figure 6. Applied/design shear and permissible shear at the 13 riprap design stations for the 10-year lining event.

3.8. Numerical Sensitivity and Structural-Control Screening

Representative checks of whether Q was approximately equal to VA were consistent with the hydraulic tables, and the HEC-15 worksheet reproduces the applied-shear equation when local bed slope is used. The numerical sensitivity screening at STA 232+00 and STA 239+00 shows that individual ±10% roughness, ±20% discharge, and ±20% friction-slope perturbations change computed water depth by no more than approximately 0.074 m, velocity by no more than approximately 7.8%, and applied boundary shear by no more than approximately 15%. The combined high-stage case (+10% n, +20% Q, −20% S) increases water depth by approximately 0.105 m at STA 232+00 and 0.150 m at STA 239+00. A separate adverse fixed-geometry screening that reduces existing-condition velocity and increases proposed-condition velocity still leaves proposed velocity approximately 31% lower at both representative locations. Detailed values are provided in Appendix B.

The omitted stair-like structure at STA 241+10 was also screened quantitatively. Over an approximate 40 ft transition length, a 10% grade represents about 4.0 ft of fall, compared with about 0.52 ft at the 1.3% approach grade; the difference is approximately 3.48 ft (1.06 m) of potential head. If expressed entirely as velocity head, this corresponds to approximately 15.0 ft/s (4.56 m/s). This value is an energy-scale indicator rather than a predicted velocity reduction, but it is large relative to the modeled 10-year velocity of 10.57 ft/s (3.22 m/s) near STA 241+50. The omission is therefore most relevant locally between approximately STA 241+10 and STA 242+00.

A terminal-control screening was performed for the documented 8 ft × 3 ft box opening. If the opening is fully occupied, mean velocity ranges from approximately 2.87 m/s for the 10-year downstream flow to 5.55 m/s for the 100-year flow. Rectangular critical depth increases from approximately 0.89 m for the 10-year event to 1.38 m for the 100-year event, exceeding the 0.91 m box rise for the 25-, 50-, and 100-year flows. For a full closed rectangular barrel, the 24 ft^2 flow area and 22 ft wetted perimeter give a hydraulic radius of approximately 1.09 ft. A full-flow Manning screening using the approximate concrete-box parameters n = 0.012–0.015 and slope = 0.02–0.04 gives barrel-friction capacities of approximately 356–630 cfs (10.1–17.8 m^3/s). The adopted 100-year downstream design flow of 437 cfs (12.37 m^3/s) therefore lies within, rather than below, the screened capacity range. For Q = 437 cfs, the required friction slope is approximately 1.93% for n = 0.012 and 3.01% for n = 0.015. Barrel-friction capacity alone therefore does not establish conveyance of the 100-year flow under all screened parameter combinations; local headwater, tailwater, entrance/exit losses, and transition to full or pressurized flow remain relevant downstream controls. Appendix B summarizes these calculations.

4. Discussion

4.1. Hydraulic Consequences of the Retrofit

The analysis shows a clear but spatially nonuniform hydraulic trade-off. The proposed reconstruction generally increases WSE while reducing channel velocity and Froude number. Similar infrastructure comparisons have reported that geometric modification can reduce local velocity without reducing overall conveyance [7,8]. In this corridor, the greatest hydraulic changes are concentrated within the reconstructed reaches rather than being distributed uniformly along the full modeled length.

The greatest changes occur inside the reconstructed reaches. Mean velocity reductions of about 54–56% within those limits are substantially larger than changes outside them. The effect should be understood as the combined influence of geometry, grade, and roughness, while the smaller changes outside the reconstruction limits represent propagated hydraulic response rather than direct geometric modification.

4.2. Water-Level and Velocity Trade-Off

The mean–median difference in WSE is central to interpretation. Median station-level increases are approximately 0.11–0.15 m, whereas the arithmetic mean is elevated by localized reconstructed sections with much larger WSE shifts. Medians, IQRs, station-level plots, and maxima therefore provide a more representative description of the spatial response than means alone. The study design indicates more than 0.91 m of 100-year freeboard, although this acceptance measure remains conditional on the adopted geometry and boundary treatment.

4.3. Station 2 and Local Flow-Regime Complexity

Station 2 is not treated as representative of the interior reach in velocity comparisons. Its 25- and 50-year existing-condition outputs combine very high velocity and Froude number with a small flow area, followed by a large flow-area expansion and subcritical response for the 100-year event. The section lies adjacent to the downstream normal-depth boundary and immediately downstream of a generic HEC-RAS culvert marker at RS 94. The non-monotonic response is therefore consistent with a boundary-adjacent control/regime transition, but the available information does not uniquely attribute the behavior to the boundary condition, local structure, geometry, or numerical regime switching. Recent work likewise shows that local hydraulic outputs can be sensitive to model dimensionality, topography, and boundary representation [12–15,29].

The stair-like structure at STA 241+10 introduces a separate local uncertainty. The screening difference between a 10% transition grade and a 1.3% approach grade over approximately 40 ft is about 1.06 m of potential head, corresponding to an equivalent velocity-head scale of approximately 4.56 m/s. The value does not represent an expected field velocity reduction because actual dissipation depends on step geometry, aeration, turbulence, and tailwater; it demonstrates that omission of the structure can materially affect local energy distribution. The principal influence zone is therefore considered to be approximately STA 241+10-242+00, and modeled velocities in this short reach should be interpreted as simplified design-scenario values.

4.4. Culvert Extension and Downstream Control

The HY-8 calculation evaluates the proposed 60 in extension only; it does not independently establish the capacity of the existing 42 in barrel or the complete 42/60 in series system. The appropriate component-level conclusion is that the larger extension did not introduce an additional modeled restriction under the 100-year check. At the downstream end, the 8 ft × 3 ft box-culvert screening indicates a parameter-dependent condition. Full-flow Manning conveyance ranges from approximately 356 to 630 cfs across the evaluated roughness and slope ranges, so the 100-year design flow of 437 cfs lies within the screened capacity envelope. Barrel-friction capacity therefore cannot be considered sufficient under every evaluated parameter combination. In addition, calculated critical depth exceeds the box rise for the 25-, 50-, and 100-year flows. Consequently, the structure may influence local headwater/backwater conditions and the transition to full or pressurized flow near the downstream model boundary. This uncertainty is concentrated near the downstream model boundary and is one reason Station 2 is interpreted separately from the interior reach.

4.5. Shear Stress and Erosion Protection

The riprap analysis confirms why velocity alone is an insufficient erosion metric. At the 60 in extension outlet, the HY-8 velocity of 5.03 m/s is similar in magnitude to the 4.84 m/s receiving-channel velocity used in the STA 232+00 lining calculation, but the two values represent different hydraulic design checks and are not treated as directly equivalent

conditions. Outlet-protection compatibility is therefore evaluated using the final controlling HEC-15 lining calculation dated 15 March 2024. At STA 232+00, RR6 with D50 = 0.457 m (18 in) provides a permissible shear of 1105.6 Pa compared with an applied shear of 663.1 Pa; after application of the adopted safety factor of 1.50, the stability ratio is 1.11. The lining therefore satisfies the adopted shear criterion, although the limited margin supports conservative interpretation and maintenance attention. The 10-year lining event remains distinct from the 50-year ditch/culvert design criterion and the 100-year extension/freeboard checks [25,26].

Several locations have comfortable margins, whereas others are close to the adopted threshold. Because the StreamStats discharges are extrapolated and no field calibration is available, thin stability margins should be viewed as design-check results rather than exact predictions of long-term performance.

4.6. Hydrologic and Parameter Uncertainty

Hydrologic uncertainty remains one of the principal limitations. The Rational Method comparison provides an independent order-of-magnitude check for the 10-year upstream flow, but it does not validate the higher return periods or provide prediction intervals outside the regression domain. The 25-, 50-, and 100-year StreamStats discharges are therefore treated as adopted design inputs, with the 50-year event representing the principal ditch/culvert design condition and the 100-year event serving as an additional stress/verification scenario [20].

Relative existing–proposed differences are internally comparable because the same adopted forcing and computational framework were used. The numerical screening shows that plausible perturbations in n, Q, and friction slope alter local depth, velocity, and shear but do not reverse the principal velocity-reduction pattern at the representative reconstructed sections. At the same time, the combined high-stage case raises local depth by as much as approximately 0.15 m, demonstrating that absolute WSE and freeboard are more sensitive quantities. The screening should therefore be interpreted as a quantitative uncertainty bound at representative sections rather than a complete model-wide uncertainty analysis.

4.7. Terrain, Calibration, and Reproducibility

Recent hydraulic studies show that terrain resolution, geometry, boundary conditions, and observational data can materially affect modeled flood depths and velocities [12–19]. No event-specific observed discharge, WSE, high-water marks, surveyed flood extents, or measured channel velocities were available for calibration or independent validation. Site photographs (Appendix A) document physical channel and structural conditions but cannot validate event hydraulics. Confidence is therefore highest in the internal existing–proposed comparison under the adopted model setup, lower in the exact magnitude of absolute WSE, velocity, freeboard, and shear, and lowest in the immediate vicinity of Station 2, the stair/drop structure, and the terminal control zone. The results are consequently interpreted as engineering scenario comparisons rather than calibrated predictions of field behavior.

4.8. Practical Engineering Implications

The case supports a practical four-step assessment sequence for constrained drainage retrofits: (1) verify adopted hydrologic inputs and their uncertainty; (2) compare station-level channel response inside and outside the reconstruction limits; (3) check structural controls such as culvert extensions without overstating what each calculation proves; and (4) evaluate erosion protection independently using local shear-based criteria. Each step should be judged against documented, site-specific design criteria. The value of the pro-

cedure is to connect these checks within one corridor assessment; application elsewhere requires local geometry, hydrology, boundary conditions, and acceptance criteria.

5. Conclusions

The analysis indicates that the proposed trail-related ditch reconstruction produces a spatially concentrated hydraulic response rather than a uniform reach-wide change. Within the reconstructed reaches, mean channel velocity is approximately 54–56% lower across the modeled events; outside those limits, changes are substantially smaller and more variable. The representative numerical sensitivity screening did not reverse this velocity-reduction pattern under the tested roughness, discharge, and friction-slope perturbations.

Across all 24 matched sections, mean velocity decreases by 34.9–44.7%, while median WSE increases by approximately 0.11–0.15 m. Local WSE increases are much larger at a small number of reconstructed sections, so medians, IQRs, and station-level profiles are more informative than means alone. In the combined high-stage sensitivity case, representative water depths increased by approximately 0.10–0.15 m, showing that absolute WSE and freeboard remain parameter-sensitive even when the direction of the velocity response is stable.

The anomalous downstream Station 2 exhibits non-monotonic velocity, depth, flow area, and Froude response and lies adjacent to the downstream normal-depth boundary and a nearby HEC-RAS culvert marker. Its behavior is consistent with a local control/regime transition, but boundary, structure, geometry, and numerical effects cannot be uniquely separated. Station 2 is therefore retained in the complete dataset but is not used as a representative interior-reach result.

The HY-8 calculation supports a component-level conclusion: the proposed 60 in extension did not introduce an additional modeled restriction at the 100-year upstream design flow, but the calculation does not independently prove the capacity of the existing 42 in barrel or the full series system. The receiving-channel protection at STA 232+00 is based on the final controlling RR6 D50 = 18 in lining calculation and satisfies the adopted HEC-15 shear criterion with an SF-adjusted stability ratio of 1.11. This lining check does not constitute a coupled outlet-jet scour analysis. The terminal 8 ft x 3 ft box-culvert screening produces a full-flow capacity range that brackets the adopted 100-year discharge rather than exceeding it under all evaluated parameter combinations. Together with the critical-depth results, this indicates that downstream control and local headwater/backwater effects remain plausible during the larger events.

The principal limitations are the absence of field calibration or independent event validation, extrapolated StreamStats discharges outside the preferred regression drainage-area range, incomplete terrain metadata, omission of the stair-like energy-dissipation structure from the 1D channel geometry, and uncertainty in the exact downstream culvert representation. The stair screening indicates a potentially important local energy scale near STA 241+10-242+00, while the terminal-control screening reinforces caution near the downstream boundary. The reported numerical results should therefore be interpreted as conditional engineering scenario responses under the adopted inputs and model configuration.

For similar constrained corridors, the transferable contribution is the assessment sequence rather than the site-specific numerical result: document hydrologic and parameter uncertainty, report actual roughness and boundary assumptions, compare station-level channel response, distinguish direct reconstruction effects from propagated changes, screen local structural controls, assess culvert components without overstating system capacity, and evaluate erosion resistance using explicit shear-based criteria.

Supplementary Materials: The following supporting information can be downloaded at https://www.mdpi.com/article/10.3390/hydrology13120314/s1: Figure S1, existing and proposed HEC-RAS longitudinal profiles; Figures S2 and S3, representative existing and proposed cross sections; Figure S4, downstream-control geometry associated with Station 2; and Figure S5, selected upstream and downstream plan/profile details showing reconstructed reaches and key hydraulic structures.

Author Contributions: Conceptualization, A.J.A., M.N.A., H.H.D. and M.M.Z.; methodology, A.J.A., H.H.D., M.N.A., M.M.Z. and N.M.H.; software, A.J.A., M.N.A. and M.M.Z.; validation, A.J.A., H.H.D., M.M.Z. and N.M.H.; formal analysis, A.J.A., H.H.D., M.N.A. and M.M.Z.; investigation, A.J.A., H.H.D., M.N.A. and M.M.Z.; resources, A.J.A. and H.H.D.; data curation, A.J.A. and M.M.Z.; writing—original draft preparation, A.J.A. and M.M.Z.; writing—review and editing, H.H.D., M.N.A., T.D. and N.M.H.; visualization, A.J.A. and M.M.Z.; supervision, A.J.A., M.N.A., N.M.H. and M.M.Z.; project administration, A.J.A. All authors have read and agreed to the published version of the manuscript.

Funding: This research received no external funding.

Data Availability Statement: The data presented in this study are available within the article. Additional raw data, model files, design calculations, and supporting study documents are not publicly available due to privacy, confidentiality, and ownership restrictions by the company. Only the data, figures, and results presented in the article are available for public use.

Acknowledgments: The authors gratefully acknowledge Crawford, Murphy & Tilly, Inc., Davenport, IA, USA, for its administrative and technical support during the preparation of this study. During the preparation of this work, the authors used ChatGPT (GPT-5.6) and Grammarly for Windows (version 1.2.314.2009) to rephrase sentences and enhance language. After using these tools/services, the authors reviewed and edited the content as needed and take full responsibility for the content of the published article.

Conflicts of Interest: Author Ahmad J. Alzubaidi is employed by Crawford, Murphy & Tilly, Inc., USA. This study is not presented as an independent third-party validation of CMT's design. Mutaz M. Zoubi is employed by the Jordan Atomic Energy Commission, Jordan. The remaining authors declare that the research was conducted in the absence of any commercial or financial relationships that could be construed as potential conflicts of interest.

Abbreviations

A	Flow cross-sectional area
AEP	Annual exceedance probability
D_{50}	Median riprap particle diameter
DEM	Digital elevation model
D_h	Hydraulic depth
Fr	Froude number
g	Gravitational acceleration
HEC-15	Federal Highway Administration guidance for roadside-channel protection
HEC-RAS	Hydrologic Engineering Center River Analysis System
HY-8	Federal Highway Administration culvert hydraulic analysis program
IDOT	Illinois Department of Transportation
LiDAR	Light Detection and Ranging
n	Manning's roughness coefficient
P_w	Wetted perimeter
Q	Discharge
R	Hydraulic radius
RP	Return period
SF	Safety factor
S_f	Energy/friction slope
T	Return period
T_w	Water-surface top width
USGS	United States Geological Survey

V	Mean flow velocity
WSE	Water-surface elevation
γ	Unit weight of water
γ_s	Unit weight of riprap stone
τ_d	Design shear stress
τ_p	Permissible shear stress

Appendix A



Figure A1. Representative field photographs from the study corridor showing the existing paved ditch, stair/drop structure, box culvert, and roadside drainage setting.

https://doi.org/10.3390/hydrology13120314

Appendix B. Hydraulic Model Reproducibility and Screening Calculations

Table A1. Manning roughness assignments and normal-depth boundary slopes used in the hydraulic model.

Scenario	Road Station/Boundary	Condition	Channel n/S	Vegetated/Grass Overbank n
Existing	STA 229+15-233+10	Concrete-lined channel	0.013	0.040–0.050
Existing	STA 233+10-237+06	Earthen/grass channel	0.030–0.035	0.040–0.050
Existing	STA 237+06-241+10	Concrete-lined channel	0.013	0.040–0.050
Existing	STA 241+10-241+50	Stair/drop transition	0.025–0.030	0.040–0.050
Existing	STA 241+50-242+38	Open-channel transition	0.030–0.035	0.040–0.050
Proposed	STA 229+15-233+10	Riprap-lined channel	0.035–0.040	0.040–0.050
Proposed	STA 233+10-237+06	Unchanged intermediate reach	0.030–0.035	0.040–0.050
Proposed	STA 237+06-241+10	Riprap-lined channel	0.035–0.040	0.040–0.050
Proposed	STA 241+10-241+50	Post-drop riprap transition	0.035–0.040	0.040–0.050
Proposed	STA 241+50-242+38	Riprap/gabion reach	0.040–0.045	0.040–0.050
Boundary	Upstream normal depth	Friction slope S	0.030 *ft*/*ft*	-
Boundary	Downstream normal depth—existing	Friction slope S	0.0245 *ft*/*ft*	-
Boundary	Downstream normal depth—proposed	Friction slope S	0.020 *ft*/*ft*	-

Table A2. Representative 10-year HEC-RAS hydraulic output at two matched locations.

Location	Condition	WSE (ft)	Area (ft2)	Top Width (ft)	Hyd. Depth A/T (ft)	V (ft/s)	Fr	E.G. Slope
RS 1254 (STA 232+00)	Existing	632.1	14.67	15	0.98	20.56	3.34	0.027397
RS 1254 (STA 232+00)	Proposed	632.47	14.24	12.55	1.13	15.87	2.63	0.134354
RS 519 (STA 239+00)	Existing	610.66	12.32	9.89	1.25	19.33	2.88	0.020264
RS 519 (STA 239+00)	Proposed	614.11	25.35	15.70	1.61	8.91	1.24	0.027264

Table A3. Numerical sensitivity screening at STA 232+00 and STA 239+00. Freeboard change is equal in magnitude and opposite in sign to the listed depth change for a fixed bank elevation.

Perturbation	STA 232+00 Δdepth (m)	ΔV (%)	Δtau (%)	STA 239+00 Δdepth (m)	ΔV (%)	Δtau (%)
n −10%	−0.025	+7.7	−5.6	−0.036	+7.7	−5.6
n +10%	+0.024	−6.5	+5.3	+0.034	−6.6	+5.3
Q −20%	−0.052	−6.4	−11.5	−0.074	−6.3	−11.5
Q +20%	+0.047	+5.5	+10.4	+0.067	+5.4	+10.4
S −20%	+0.028	−7.6	−15.0	+0.040	−7.6	−15.0
S +20%	−0.022	+6.6	+14.2	−0.031	+6.7	+14.2
Combined: n +10%, Q +20%, S −20%	+0.105	−9.0	−1.3	+0.150	−9.1	−1.4

Table A4. Terminal 8 ft × 3 ft box-culvert hydraulic screening using the downstream design discharges.

Return Period (yr)	Q, cfs (m3/s)	Velocity if the 24 ft2 Opening Is Full, ft/s (m/s)	Rectangular Critical Depth, ft (m)	yc/3 ft Rise
10	226 (6.40)	9.42 (2.87)	2.92 (0.89)	0.97
25	310 (8.78)	12.92 (3.94)	3.60 (1.10)	1.20
50	370 (10.48)	15.42 (4.70)	4.05 (1.23)	1.35
100	437 (12.37)	18.21 (5.55)	4.53 (1.38)	1.51

Table A5. Stair/drop energy-scale screening near STA 241+10.

Screening Quantity	Value
Approximate transition length	40 ft (12.2 m)
Approach grade	1.3%
Steep transition grade	10%
Fall over 40 ft at 1.3%	0.52 ft (0.16 m)
Fall over 40 ft at 10%	4.00 ft (1.22 m)
Difference in potential head	3.48 ft (1.06 m)
Equivalent velocity-head scale sqrt(2 gΔH)	15.0 ft/s (4.56 m/s)
10-year modeled velocity near STA 241+50	10.57 ft/s (3.22 m/s)

Table A6. Source-based crosswalk between HEC-RAS river stations and roadway stationing for the 24 matched sections.

HEC-RAS RS	Road Station	Spatial Group
1358	231+00	Reconstructed
1307	231+50	Reconstructed
1254	232+00	Reconstructed
1202	232+50	Reconstructed
1149	233+00	Reconstructed
1097	233+50	Outside
1044	234+00	Outside
992	234+50	Outside
939	235+00	Outside
887	235+50	Outside
835	236+00	Outside
782	236+50	Outside
729	237+00	Outside
675	237+50	Reconstructed
622	238+00	Reconstructed
570	238+50	Reconstructed
519	239+00	Reconstructed
468	239+50	Reconstructed
417	240+00	Reconstructed

Table A6. *Cont.*

HEC-RAS RS	Road Station	Spatial Group
367	240+50	Reconstructed
317	241+00	Reconstructed
266	241+50	Reconstructed
215	242+00	Reconstructed
2	Downstream terminus near STA 244+02	Outside

References

1. Nodine, T.G.; Conley, G.; Riihimaki, C.A.; Holland, C.; Beck, N.G. Modeling the impact of future rainfall changes on the effectiveness of urban stormwater control measures. *Sci. Rep.* **2024**, *14*, 4082. [CrossRef]
2. Anwer, A.A.; Soliman, A.H.; Radwan, H.G. Hydraulic-based optimization algorithm for the design of stormwater drainage networks. *Appl. Water Sci.* **2024**, *14*, 139. [CrossRef]
3. Khatooni, K.; Hooshyaripor, F.; MalekMohammadi, B.; Noori, R. A new approach for urban flood risk assessment using coupled SWMM-HEC-RAS-2D model. *J. Environ. Manag.* **2025**, *374*, 123849. [CrossRef]
4. Chen, W.; Wu, H.; Kimball, J.S.; Alfieri, L.; Nanding, N.; Li, X.; Jiang, L.; Wu, W.; Tao, Y.; Zhao, S.; et al. A coupled river basin-urban hydrological model (DRIVE-Urban) for real-time urban flood modeling. *Water Resour. Res.* **2022**, *58*, e2021WR031709. [CrossRef]
5. Guo, K.; Guan, M.; Yan, H.; Xia, X. A spatially distributed hydrodynamic model framework for urban flood hydrological and hydraulic processes involving drainage flow quantification. *J. Hydrol.* **2023**, *625*, 130135. [CrossRef]
6. Rohith, A.N.; Sudheer, K.P. A novel safe-fail framework for the design of urban stormwater drainage infrastructures with minimal failure and flood severity. *J. Hydrol.* **2023**, *627*, 130393. [CrossRef]
7. Schilling, K.E.; Anderson, E.S.; Cintura, I.; Eustace, B.S.; Arenas Amado, A. Modeling the potential of a roadside two-stage ditch to reduce flooding and erosion risks. *Hydrology* **2026**, *13*, 220. [CrossRef]
8. Alzubaidi, A.J.; Darwish, H.H.; Zoubi, M.M.; Abu-Afifeh, Q.Y.; Al-Rkebat, R.; Al-Jawaldeh, H.F.; Obeidat, N.; Al-Nawaiseh, T.M.F.; Brezat, A.; Al-Omari, S.; et al. Hydraulic and scour assessment for sustainable bridge replacement over the Mid Fork Saline River, USA. *Infrastructures* **2026**, *11*, 253. [CrossRef]
9. Mohamed, A.; Katambara, Z. Evaluating the hydraulic performance and sustainability of the Simike-Nzovwe roadside drainage system in Mbeya City, Tanzania, using HEC-RAS modelling. *Asian J. Water Environ. Pollut.* **2025**, *22*, 240–248. [CrossRef]
10. Bagiouk, S.S.; Agiou, A.E.; Katsifarakis, K.L. Urban runoff simulation using HEC-RAS and the Modified Rational Method. *Water Resour. Manag.* **2026**, *40*, 329. [CrossRef]
11. Iroume, J.Y.-A.; Onguéné, R.; Djanna Koffi, F.; Colmet-Daage, A.; Stieglitz, T.; Essoh Sone, W.; Bogning, S.; Olinga Olinga, J.M.; Ntchantcho, R.; Ntonga, J.-C.; et al. The 21st August 2020 flood in Douala (Cameroon): A major urban flood investigated with 2D HEC-RAS modeling. *Water* **2022**, *14*, 1768. [CrossRef]
12. Arash, A.M.; Yasi, M. The assessment for selection and correction of RS-based DEMs and 1D and 2D HEC-RAS models for flood mapping in different river types. *J. Flood Risk Manag.* **2023**, *16*, e12871. [CrossRef]
13. Costabile, P.; Costanzo, C.; Ferraro, D.; Barca, P. Is HEC-RAS 2D accurate enough for storm-event hazard assessment? Lessons learnt from a benchmarking study based on rain-on-grid modelling. *J. Hydrol.* **2021**, *603*, 126962. [CrossRef]
14. Moghim, S.; Ahmadi Gharehtoragh, M.; Safaie, A. Performance of the flood models in different topographies. *J. Hydrol.* **2023**, *620*, 129446. [CrossRef]
15. Fikri, R.M.; Herawati, H.; Pranoto, W.A. Influence of DEM spatial resolution on the accuracy and computational efficiency of HEC-RAS 1D and 2D flood inundation modelling. *Water* **2026**, *18*, 1203. [CrossRef]
16. Shrestha, A.; Garcia, M.; Doerry, E. Leveraging catchment scale automated novel data collection infrastructure to advance urban hydrologic-hydraulic modeling. *Environ. Model. Softw.* **2024**, *178*, 106046. [CrossRef]
17. Huang, Y.; Zhang, J.; Zheng, F.; Jia, Y.; Kapelan, Z.; Savic, D. Exploring the performance of ensemble smoothers to calibrate urban drainage models. *Water Resour. Res.* **2022**, *58*, e2022WR032440. [CrossRef]
18. Hu, C.; Xia, J.; She, D.; Jing, Z.; Hong, S.; Song, Z.; Wang, G. Parameter regionalization with donor catchment clustering improves urban flood modeling in ungauged urban catchments. *Water Resour. Res.* **2024**, *60*, e2023WR035071. [CrossRef]
19. Assaf, M.N.; Salis, N.; Manenti, S.; Tamellini, L.; Creaco, E.; Todeschini, S. Optimizing hydrological modelling on real urban catchment: Impact of calibration data selection and objective function. *J. Hydrol.* **2025**, *662*, 133821. [CrossRef]
20. Over, T.M.; Marti, M.K.; O'Shea, P.S.; Sharpe, J.B. *Estimating Peak-Flow Quantiles for Selected Annual Exceedance Probabilities in Illinois*; Research Report FHWA-ICT-23-014; Illinois Center for Transportation: Rantoul, IL, USA, 2023. [CrossRef]

21. Khan, S.T.; Wynn-Thompson, T.; Sample, D.J. Stormwater controls for channel stability: Focusing on bed material transport prevents degradation. *J. Environ. Manag.* **2025**, *374*, 123651. [CrossRef]
22. Aness, W.T.; Hadadin, N.A.; Zoubi, M.M.; Abu-Afifeh, Q.Y.; Al-Afeshat, A.F.; Al-Jawaldeh, H.F.; Qutishat, T.A.; AlHalaigah, M.R.; Alnizami, N.H.; Aljarrah, A.; et al. Runoff and sediment dynamics modeling for erosion risk reduction and sustainable watershed management. *Glob. J. Environ. Sci. Manag.* **2026**, *12*, 813–836. [CrossRef]
23. Abu-Afifeh, Q.; Rahbeh, M.; Al-Afeshat, A.; Al-Omari, S.; Qutishat, T.A.; Brezat, A.; Alkayed, A. Dam sustainability's interdependency with climate change and dam failure drivers. *Sustainability* **2023**, *15*, 16239. [CrossRef]
24. Crawford, Murphy & Tilly, Inc. *Location Drainage Study—River-to-River Trail*; Job No. 22004369.00; Prepared for the City of Moline: Moline, IL, USA, 2024.
25. Kilgore, R.T.; Cotton, G. *Design of Roadside Channels with Flexible Linings*, 3rd ed.; Hydraulic Engineering Circular No. 15; FHWA-NHI-05-114; Federal Highway Administration: Washington, DC, USA, 2005.
26. Illinois Department of Transportation. *Drainage Manual*; Chapter 5 used for open-channel and floodplain roughness procedures; Section 9.500 used for roadside-channel lining design criteria; Bureau of Design and Environment: Springfield, IL, USA, 2011.
27. U.S. Army Corps of Engineers, Hydrologic Engineering Center. *HEC-RAS River Analysis System, Version 6.5: Hydraulic Reference Manual and User's Manual*; U.S. Army Corps of Engineers, Hydrologic Engineering Center: Davis, CA, USA, 2024.
28. Federal Highway Administration. *HY-8 Culvert Hydraulic Analysis Program*; Version 8.0.0 (build date 29 May 2024); U.S. Department of Transportation: Washington, DC, USA, 2024.
29. Kohanpur, A.H.; Saksena, S.; Dey, S.; Johnson, J.M.; Riasi, M.S.; Yeghiazarian, L.; Tartakovsky, A.M. Urban flood modeling: Uncertainty quantification and physics-informed Gaussian processes regression forecasting. *Water Resour. Res.* **2023**, *59*, e2022WR033939. [CrossRef]

Disclaimer/Publisher's Note: The statements, opinions and data contained in all publications are solely those of the individual author(s) and contributor(s) and not of MDPI and/or the editor(s). MDPI and/or the editor(s) disclaim responsibility for any injury to people or property resulting from any ideas, methods, instructions or products referred to in the content.